Heliyon 10 (2024) e28693

Contents lists available at ScienceDirect

Heliyon

journal homepage: www.cell.com/heliyon

Research article

Mechanism of acacetin regulating hepatic stellate cell apoptosis based on network pharmacology and experimental verification

Xue Hu [a,1], Haotian Shen [a,1], Rong Liu [a], Bin Tang [b], Fengmei Deng [a,*]

[a] School of Basic Medical Science, Chengdu Medical College, Chengdu, 610500, China
[b] Clinical Medical College and The First Affiliated Hospital of Chengdu Medical College, Chengdu, 610500, China

ARTICLE INFO

Keywords:
Acacetin$_1$
Apoptosis$_2$
Hepatic fibrosis$_3$
Molecular Docking$_4$
Network Pharmacology$_5$

ABSTRACT

Background: Hepatic fibrosis is caused by various liver diseases and eventually develops into liver cancer. There is no specific drug approved for the treatment of hepatic fibrosis in the world. Acacetin (AC), a natural flavonoid, is widely present in nature in various plants, such as black locust, Damiana, Silver birch. It has been reported that acacetin can inhibit the proliferation of cancer cells and induce apoptosis.

Purpose: In this study, we investigated the effect of acacetin on hepatic stellate cell apoptosis, thereby improving hepatic fibrosis, and combined experimental validation and molecular docking to reveal the underlying mechanism.

Result: First, we discovered that acacetin inhibited hepatic stellate cell proliferation as well as the expression of fibrosis-related proteins α-smooth muscle actin (α-SMA) and collagen type I 1 gene (COL1A1) in LX2 cells. Acacetin was then found to promote apoptosis of hepatic stellate cells through the caspase cascade pathway. Network pharmacology screening showed that TP53, CASP3, CASP8, BCL2, PARP1, and BAX were the most important targets related to apoptosis in the PPI network. GO and KEGG analyses of these six important targets were performed, and the top 10 enriched biological processes and related signaling pathways were revealed. Further network pharmacology analysis proved that apoptosis was involved in the biological process of acacetin's action against hepatic stellate cells. Finally, molecular docking revealed that acacetin binds to the active sites of six apoptotic targets. In vitro experiments further confirmed that acacetin could promote the apoptosis of LX2 cells by inducing the activation of P53, thereby improving hepatic fibrosis.

Conclusion: acacetin induces P53 activation and promotes apoptosis of hepatic stellate cells thereby ameliorating hepatic fibrosis.

1. Introduction

Hepatic fibrosis is an intermediate process in the transformation of various liver diseases into hepatocellular carcinoma [1]. The activation of hepatic stellate cells (HSCs) into myofibroblasts is the main cause of hepatic fibrosis [2]. HSCs are highly activated after liver injury, leading to the proliferation and overexpression of the extracellular matrix (ECM) [3], moreover, a large number of phenotypic proteins α-SMA and COL1A1 of liver fibrosis are released, which promote the formation of collagen fibers and lead to liver

* Corresponding author. Chengdu Medical College, 783 Xindu Dadao, Xindu District, Chengdu City, Sichuan Province, China.
E-mail address: dengfengmei123@cmc.edu.cn (F. Deng).
[1] These authors contributed equally to this work.

https://doi.org/10.1016/j.heliyon.2024.e28693
Received 25 June 2023; Received in revised form 21 March 2024; Accepted 22 March 2024

fibrosis and liver cancer [4], α-SMA and COL1A1 as marker proteins of liver fibrosis, they are often used to detect the degree of liver fibrosis. Therefore, in this study, we mainly examined the expression of these two fibrosis marker proteins in LX-2 cells. In China, the incidence of hepatic fibrosis is increasing year by year, and the age of onset also tends to be younger [5]. While early hepatic fibrosis is reversible, as long as it is not in the late stage, there is still the possibility of reversal [6]. However, there is no specific drug for the treatment of hepatic fibrosis [7]. Therefore, new pharmacological molecules or strategies for the treatment of hepatic fibrosis are urgently needed to improve patient survival.

Traditional hepatoprotective drugs have complex components and low specificity, but TCM monomer has low side effects and high specificity. Acacetin (5,7-dihydroxy-4′-methoxyflavone, AC) is a natural flavonoid TCM monomer that is widely found in various plants [8], such as black locust, Damiana, Silver birch [9]. Acacetin has a variety of biological functions, including anti-inflammation and anti-oxidation, and can inhibit the growth of most cancer cells and promote their apoptosis [9]. Several studies have demonstrated the pro-apoptotic activity of acacetin in vitro and in vivo. For example, acacetin was shown to inhibit cell proliferation and induce apoptosis in human HCC cell lines by inhibiting STAT3 activation [10], and M3R-associated calcium signaling and caspase-3 activation to induce apoptosis in HNSCC cells [11]. Moreover, acacetin has been shown to activate the mitochondrial caspase cascade to induce apoptosis [12]. These results suggest that acacetin has the biological function of promoting apoptosis. Apoptosis plays a necessary role in the removal of abnormal cells. Apoptosis can be triggered by both exogenous and endogenous pathways [13]. During the proapoptotic process, proapoptotic proteins CASP3, CASP8, CASP9, PARP1, and BAX are highly expressed, while anti-apoptotic protein BCL2 is low expressed. And P53 is an intracellular transcription factor, an important tumor suppressor gene, and a pro-apoptotic factor [14]. The most prominent result of p53 activation is apoptosis. Under normal conditions, a small amount of apoptosis protein is expressed in hepatic stellate cells. Therefore, promote the expression of apoptosis protein in activated hepatic stellate cells can improving liver fibrosis. However, it is still unclear whether acacetin can induce apoptosis of hepatic stellate cells by regulating P53.

Network pharmacology is an effective method to screen drug disease targets and predict possible underlying mechanisms through bioinformatics analysis [15]. For example, based on network pharmacology and experimental validation analysis, acacetin can fight sepsis through multiple targets and pathways [16]. Acacetin was shown to be a key component in Weishu decoction and could alleviate gastrointestinal motility disorders by inhibiting the activation of the PI3K-AKT signaling pathway by network pharmacology analysis [17]. In this study, we used network pharmacology combined with molecular docking and experimental validation (The measurement parameters including α-SMA, COL1A1, CASPASE-3, -8, -9, BAX, BCL2, PARP1 and TP53) to investigate the potential targets of acacetin in hepatic fibrosis and to verify the regulatory mechanism by which acacetin improves hepatic fibrosis.

2. Materials and methods

2.1. Reagent

Acacetin was purchased from MedChemExpress (No: HY-N0451), and Platelet-derived growth factor-BB (PDGF-BB) (MedChemExpress, No: HY-P7055) was purchased from Novus PDGF-BB, as the activator of HSCs, mimics the liver fibrosis microenvironment and maintains the activation state of HSCs [18].

2.2. Culture and treatment of hepatic stellate cells

LX-2 cells (Wuhan Prosay Co.) were cultured in Dulbecco's modified Eagle's medium-high (DMEM) (MedChemExpress, No: HY-K3001) medium containing 10% fetal bovine serum (MedChemExpress, No: HY-P2352), and cultured in a cell culture dish in a 5% CO2 incubator at 37 °C. Cell growth status and density were observed every day, and the cells were timely passed and replaced with new medium [18]. Then, according to the experimental requirements, AC (0, 20, 40, 60, 80 μM) and 40 ng/mL of PDGF-BB were added in each well according to the set concentration. After 24–72 h of intervention, the corresponding experimental operation was carried out.

2.2.1. Cell viability assay

Cell viability was measured according to the Cell Counting Kit-8 (CCK-8) specification protocol [19] (Bryotime, No: C0038). Cells were seeded at a density of 1×10^3 in 96-well plates and incubated at 37 °C with AC (0, 20, 40, 60, 80 μM) for 24–72 h. Subsequently, the absorbance at 450 nm wavelength was measured using a microplate reader (Thermo, MA, USA). The IC50 value (50% inhibitory concentration) was calculated, and the experimental concentration gradient of drugs was set before and after IC50.

2.2.2. Colony formation assay

Colony formation assays were performed to assess the antiproliferative activity of acacetin in hepatic fibrosis [20]. Cells were seeded in six-well plates at a density of 1000 cells per well and cultured with PDGF-BB and different concentrations of acacetin for about 10–14 days until cells grew into visible colonies. Colonies consisting of at least 50 cells are stained with 0.1% crystal violet (Beijing Solaibao Technology, No: C8470) and after the photo is taken, image J is used to count cells containing more than 50 cells [21].

2.2.3. Western blot

Cells were seeded in six-well plates at a density of 5×10^5, after 24h of acacetin treatment, the cells were lysed with RIPA (radio Immunoprecipitation Assay) (Beijing Solaibao Technology, No: R0010) containing a mixture of protease and phosphatase inhibitors

[22]. Protein concentrations were quantified using the BCA (bicinchoninic acid) protein assay (Beijing Solaibao Technology, No: PC0020) according to the manufacturer's instructions. COL1A1 and α-SMA etc. antibodies used in the Western blot assay were all sourced from Cell Signaling Technology, USA. The cells were then probed for 1 h at room temperature with horseradish peroxidase labeled anti-rabbit (1:2000) or anti-mouse (1:2000). The bound immune complexes were assayed using ChemiDoc XRS (BioRad, USA).

2.2.4. Immunofluorescence (IF)

Using the method used to measure immunofluorescence [23], the samples were purified with Cleaved-Caspase-3 (1:100; Cell Signaling Technology, No: #9661), a-smooth muscle actin (a-SMA; 1:200; Cell Signaling Technology, No: #19245), and collagen type 1-A1 (COL1A1; 1:100; Cell Signaling Technology, No: #72026) antibodies. The cell slides were then placed under an Olympus BX63 fluorescence microscope for observation.

2.2.5. Flow cytometry apoptosis analysis

In order to measure the apoptosis induced by acacetin, apoptotic cells were measured using an Annexin V-FITC apoptosis detection kit [24] (Beyotime, No: #C1062 M). LX-2 cells were cultured at a density of 1×10^5 in six-well plates and treated with different concentrations of acacetin for 24 h according to the experimental grouping. The results of cell staining were analyzed by flow cytometry (ACEA Biosciences) after staining cells according to the product instructions.

2.2.6. ROS detection

ROS production was analyzed by DCFH-DA staining by flow cytometry [25] (Solarbio, No: #CA1410). Cells were seeded at a density of 5×10^4 in six-well plates and treated with acacetin in a dose-dependent manner. According to the manufacturer's protocol, after treating cells with acacetin, the fluorescence signal intensity of ROS is analyzed by flow cytometry.

2.3. MMP measurement

Check for changes in MMP (mitochondrial membrane potential) with the JC-1 Assay Kit [26] (Solarbio, No: #M8650) according to the manufacturer's instructions, A total of 5×10^4 cells were seeded in 6-well plates, and LX-2 cells were treated with acacetin at various concentrations for 24 h. Then, after incubation according to the manufacturer's instructions, the samples were analyzed by flow cytometry.

2.4. Tunel staining

Slides were placed in 24-well plates and seeded at a density of 5×10^3 cells. After 24h treatment with different concentrations of acacetin, cells were stained according to the instructions provided by the TUNEL apoptosis detection kit [27] (Beyotime, No: #C1086). The cell slides were then placed under an Olympus BX63 fluorescence microscope for observation.

2.4.1. Quantitative RT-PCR

Total RNA was extracted using a total RNA extraction kit (Solarbio, No: R1200), and cDNA was synthesized from total RNA using an iScript cDNA synthesis kit [28] (Bio-Rad, Hercules, CA, USA), The Reaction system was 20 μL: Total RNA 1 μg, Iscript Reaction Transcription 1 μL, 5 × mix 4 μL, Free nucledase dH2O for constant volume. Gene primer sequences were synthesized by QinKe (Chengdu, China) and qPCR was performed using SYBR Green Supermix (Bio-Rad). The reaction system was 10 μL: SSoAdvanced SYBR Green Supermix 5 μL, upstream and downstream primer 0.5 + 0.5 μL, cDNA 1 μL, Nuclease-freeH2O 3 μL. The reaction conditions were

Table 1
Gene primer sequence.

Gene	Sequence
Human ACTA2	Fw 5′-CTATCCAGGCGGTGCTGTCTCT-3′ Rv 5′-GCCACGCTCAGTCAGGATCTTC-3′
Human BAX	Fw 5′-CCTCAGGATGCGTCCACCAAGA-3′ Rv 5′-TGTGTCCACGGCGGCAATCA-3′
Human BCL-2	Fw 5′-TTCGCCGAGATGTCCAGCCA-3′ Rv 5′-GCATCCCAGCCTCCGTTATCCT-3′
Human COL1A1	Fw 5′-TTTGGATGGTGCCAAGGGAG-3′ Rv 5′-CACCATCATTTCCACGAGCA-3′
Human CASP3	Fw 5′-GCCGTGGTACAGAACTGGACTG-3′ Rv 5′-AACCAGGTGCTGTGGAGTATGC-3′
Human CASP8	Fw 5′-CCTGAGCCTGGACTACATTCCG-3′ Rv 5′-CCTGCCTGGTGTCTGAAGTTCC-3′
Human CASP9	Fw 5′-CGAACTAACAGGCAAGCAGCAA-3′ Rv 5′-TCAAGAGCACCGACATCACCAA-3′
Human GAPDH	Fw 5′-GGAGCGAGATCCCTCCAAAAT-3′ Rv 5′- GGCTGTTGTCATACTTCTCATGG-3′
Human TP53	Fw 5′-GGCTCTGACTGTACCACCATCC-3′ Rv 5′-GGCACAAACACGCACCTCAAAG-3′

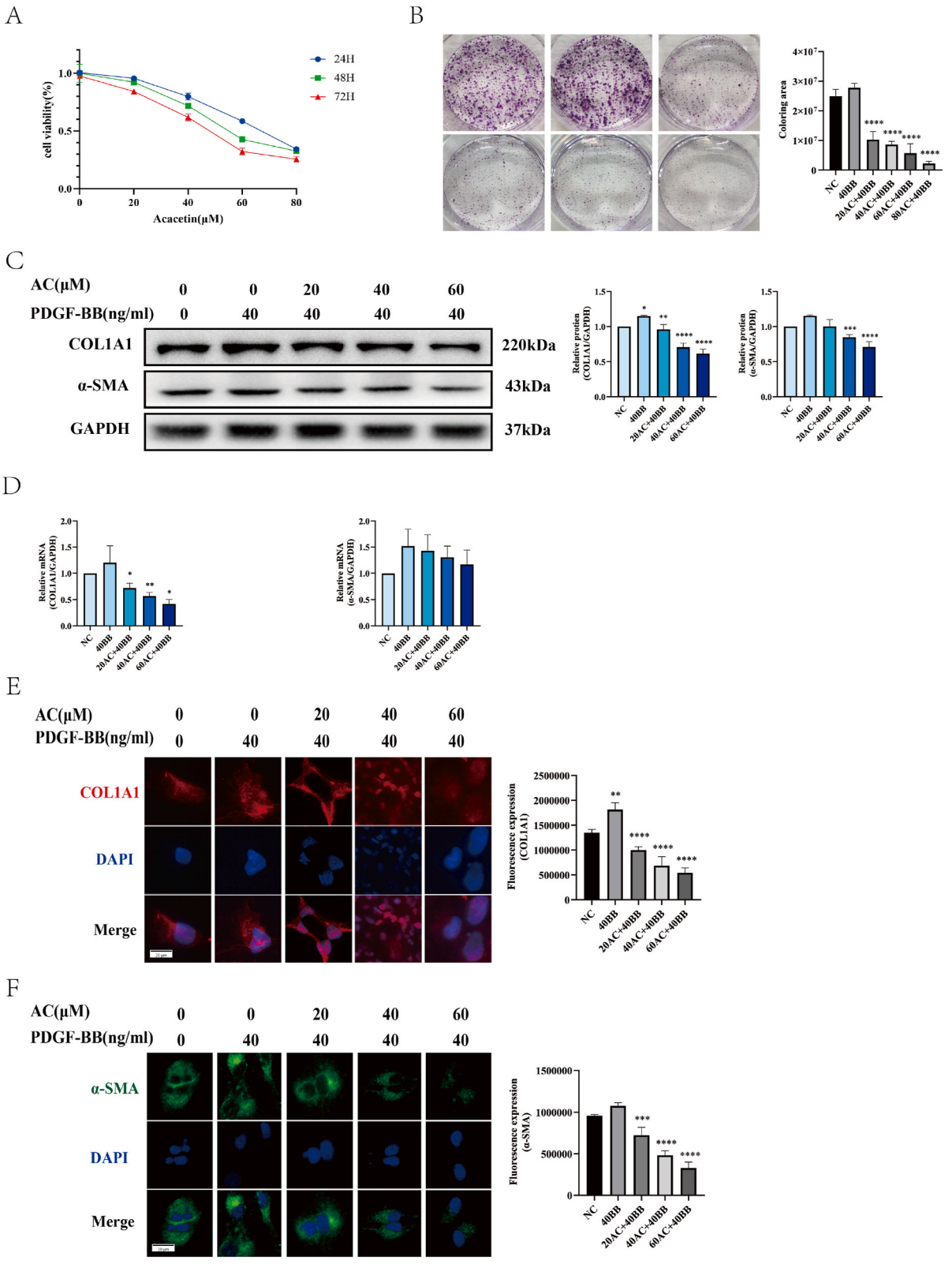

(caption on next page)

Fig. 1. Acacetin inhibits the expression of hepatic fibrotic protein. (**A**)The effect of AC on the viability of LX-2 cells was determined by CCK-8. (**B**) A colony formation assay was used to determine the anti-proliferative effect of AC on LX-2. (**C**) The expression levels of the hepatic fibrosis phenotypes COL1A1 and -SMA were determined using Western blotting. (**D**) The COL1A1 and α-SMA gene expression levels were determined using QPCR. Immunofluorescence was used to determine the intracellular expression of COL1A1 and α-SMA in (**E**) and (**F**). The data is presented as mean SEM (n = 3). The PDGF-BB stimulation group was compared with the control NC group, and the acacetin drug group was compared with the PDGF-BB stimulation group. Results to $^{*}P < 0.05$, $^{**}P < 0.01$, $^{***}P < 0.001$, $^{****}P < 0.0001$.

95 °C for 30 s. 95 °C, 15 s; 60 °C, 30 s; 40 cycles. The length of the primer is between 100 and 300 bp, and the Tm value is between 55 and 65 °C. GAPDH was used as the internal control to normalize for differences in the amount of total RNA in each sample. The sequence of relevant primers in this experiment is shown in Table 1.

2.4.2. Network pharmacology approach

Various websites were searched for the targets of action of the active ingredients in acacetin, and potential targets of liver fibrosis were screened [29]. Subsequently, a visualized acacetin-target network was established using Cytoscape v3.9.1. The common targets of acacetin and liver fibrosis were collected, and the protein-protein interaction (PPI) network was constructed using the String database as the main components of the treatment of HF. The key biological targets were obtained by counting the number of connections at each node. Use the DAVID Database website to understand the biological significance behind the large list of genes and high-throughput transcriptome and genome data that were used to identify these potential mechanisms. The common targets of acacetin and liver fibrosis were input into the DAVID database for GO analysis and KEGG pathway analysis. According to the KEGG analysis results, Cytoscpae v3.9.1 was applied to construct the acacetin-target-pathway network. The network construction revealed the characteristics of multiple targets and multiple pathways of acacetin against liver fibrosis.

2.4.3. Molecular docking

TP53 (PDB code: 1GZH), CASP3 (PDB code: 1GFW), CASP8 (PDB code: 1F9E), and BCL2 (PDB code: 1) were obtained from the Protein PDB database (https://www.rcsb.org/) under the code 1G5M, and the 3D crystal structures of PARP1 (PDB code: 3OD8) and BAX (PDB code: 6WH0) were obtained from the Protein PDB [30]. Obtain the acacia 3D structure from the TCMSP database (https://old.tcmsp-e.com/index.php). Open-source PyMOL v2.5.0 software was used to remove all non-acceptor atoms, including water, ions, and heterozygous compounds, to prepare pure protein structures. Docking experiments were subsequently performed using AutoDockTool v1.5.7 with receptor-ligand interactions to determine the site where the lowest-energy hydrogen bond binds to the residue. The binding results were visualized as 3D and pocket structure diagrams using open-source PyMOL v2.5.0.

2.5. Statistical analysis

Statistical evaluations were performed using the GraphPad Prism 8 package (GraphPad Software Inc., San Diego, CA, United States). Multiple comparisons were performed by one-way ANOVA followed by Tukey's post hoc significant difference test P values less than 0.05 indicate statistical significance.

3. Results

Acacetin can inhibit the proliferation of LX-2 cells and the expression of fibrosis-related proteins α-SMA and COL1A1.

To investigate the anti-proliferative effect of acacetin on LX-2 cells, CCK-8 was used to measure cell viability. Compared with the control group, the viability of LX-2 cells was significantly inhibited with the increase in drug concentration in a dose- and time-dependent manner (Fig. 1A). Platelet-derived growth factor BB is a drug that promotes the division and differentiation of fibroblasts. PDGF-BB was used to model LX-2 cells. A colony formation assay confirmed that under the combined action of PDGF-BB and acacetin, PDGF-BB could promote the proliferation and division of LX-2 cells. Compared with the model group, the number of colonies in the acacetin group was significantly reduced in a dose-dependent manner($P < 0.05$) (Fig. 1B). The fibrosis-related proteins α-SMA and COL1A1 were detected using Western blot, real-time PCR, and immunofluorescence. The model group could promote the expression of fibrosis-related proteins, while the acacetin group was lower than the model group ($P < 0.05$) (Fig. 1C–F).

Acacetin induces apoptosis of LX-2 cells through a caspase-dependent pathway.

To confirm whether mitochondria are involved in acacetin-induced apoptosis, the fluorescent mitochondrial probe JC-1 was used to measure mitochondrial membrane potential. The fluorescence signal in the acacetin group increased sharply in a concentration-dependent manner compared to the model group ($P < 0.05$) (Fig. 2A). Flow cytometry using annexin V-FITC staining showed that the proportion of LX-2 cells undergoing early and late apoptosis in the acacetin group was increased in a dose-dependent manner compared with the model group ($P < 0.05$) (Fig. 2B). Western blotting and real-time PCR were then used to detect the expression of related apoptotic proteins and genes in LX-2 cells treated with acacetin. At the protein level, we found that the expression of cleaved caspase-3, -8, -9, and Bax was significantly increased, while the expression of the anti-apoptotic protein Bcl-2 was decreased. The results of real-time PCR were consistent with those of a Western blot ($P < 0.05$) (Fig. 2C–D). The results of the Cleaved-Caspase3 immunofluorescence assay showed that the number of apoptotic cells in the acacetin group was significantly higher than that in the model group in a dose-dependent manner ($P < 0.05$) (Fig. 2E). These data suggest that acacetin induces mitochondrial depolarization and promotes caspase cascade activation to induce apoptosis in LX-2 cells.

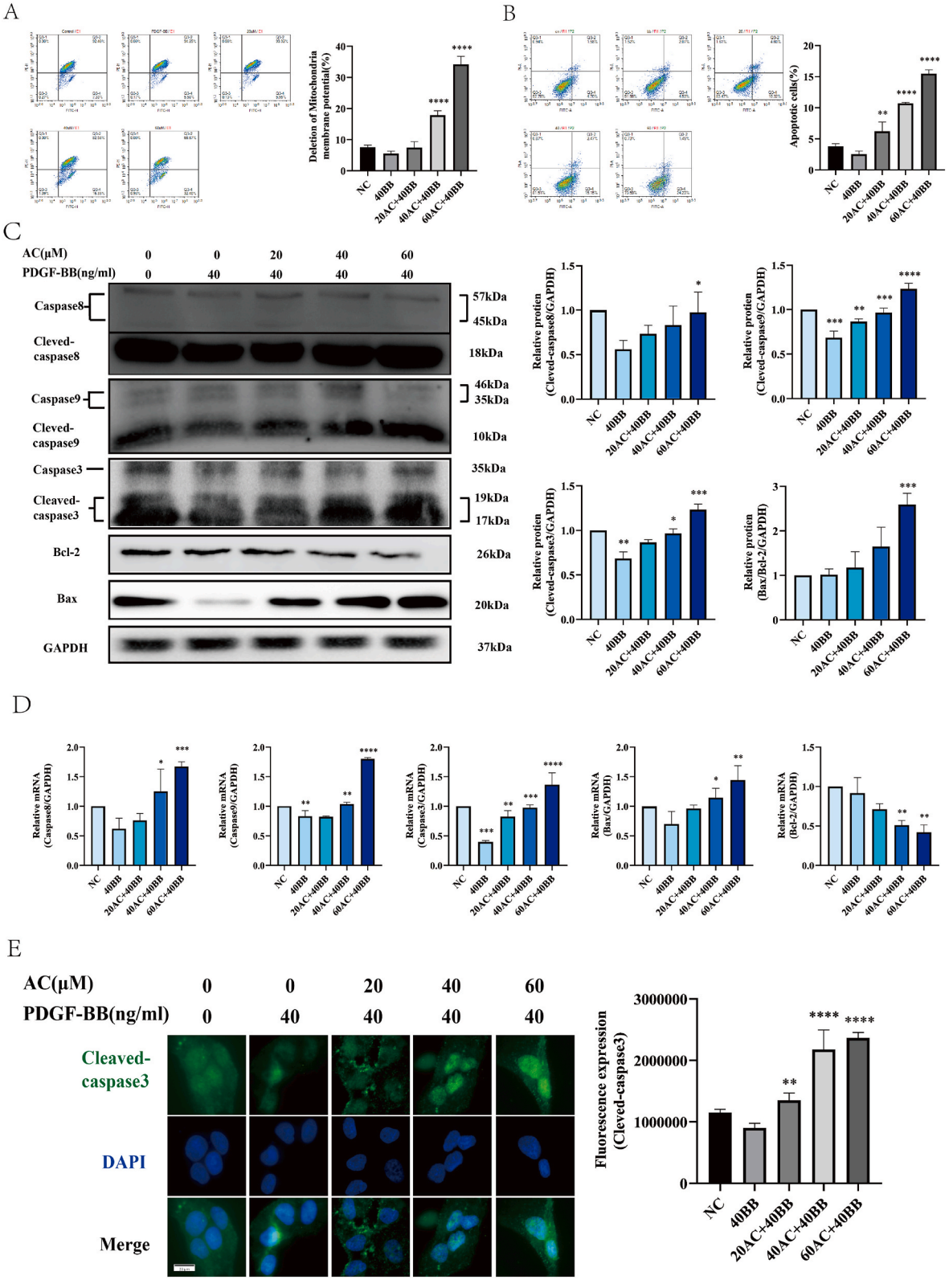

(caption on next page)

Fig. 2. Acacetin induces apoptosis of LX-2 cells through a caspase-dependent pathway. (**A**) The level of mitochondrial membrane potential loss was determined by JC-1. (**B**) The level of apoptosis was determined by FTIC. (**C**) Western blotting was used to detect the expression of apoptosis-related proteins. Cleved-caspase-8, -9, -3, Bcl-2, and Bax. (**D**)QPCR was used to measure the gene expression levels of caspase8, -9, -3, Bax, and Bcl-2. (**E**) An immunofluorescence assay was used to detect the expression of Cleved-caspase 3. The data is presented as mean SEM (n = 3). The PDGF-BB stimulation group was compared with the control NC group, and the acacetin drug group was compared with the PDGF-BB stimulation group. Results to * $P < 0.05$, ** $P < 0.01$, *** $P < 0.001$, **** $P < 0.0001$.

Acacetin induces apoptosis in LX-2 cells through a caspase-independent pathway, accompanied by ROS generation and P53 activation.

ROS are highly bioactive, and excessive amounts of ROS can cause oxidative damage to lipids, proteins, and DNA [31]. Analysis of ROS production in the cells by DCFH-DA staining of flow cytometry demonstrated that the cell fluorescence signal in the acacetin group increased sharply in a concentration-dependent manner, suggesting that the induction of ROS may activate DNA damage and lead to apoptosis in LX-2 cells ($P < 0.05$) (Fig. 3A). TUNEL staining (green fluorescence) showed that the number of nuclear apoptotic cells in LX-2 cells treated with acacetin increased in a dose-dependent manner ($P < 0.05$) (Fig. 3B). Western blot and real-time PCR showed that the expression of the DNA repair enzymes PARP1 and P53 was increased in the acacetin group ($P < 0.05$) (Fig. 3C–D). These experimental data suggest that acacetin can induce apoptosis in LX-2 cells through a caspase-independent pathway, accompanied by ROS generation and P53 activation.

Network pharmacology was used to screen the relationship and mechanism between acacetin and the common core targets of hepatic fibrosis.

After entering the standard string of acacetin into the CTD database, ETCM database, HERB database, HIT database, and TCMSP database, the targets of acacetin were determined, and 164 potential drug targets were found. A total of 1398 potential targets of hepatic fibrosis were screened by the DisGeNET database and the GeneCards database (Fig. 4A). Acacetin - hepatic fibrosis target The Venn diagram contains 70 common targets (Fig. 4A). Based on the minimum interaction score screening, a PPI network of 70 common targets between acacetin and hepatic fibrosis was constructed, and the apoptosis-related targets TP53 (TP53 gene, also known as P53, is a tumor suppressor gene. Simply put, TP53 and P53 are the same), CASP3, CASP8, BCL2, PARP1, and BAX were identified as the core targets (Fig. 4B). GO and KEGG analyses were performed, and the core targets TP53, CASP3, CASP8, BCL2, PARP1, and BAX were entered into the DAVID database to clarify the possible mechanism of acacetin affecting hepatic fibrosis. GO analysis of BP terms revealed that six core targets were mainly related to pro-apoptotic processes, response to LPS, etc (Fig. 4C). GO analysis of the CC terms revealed that six core targets were found to be mainly related to double-strand break sites, pore complexes, nuclear plasma, and other cellular components (Fig. 4D). GO analysis of MF terms showed that the six core targets were mainly related to molecular functions such as ubiquitin protein lipase binding, protein phosphatase 2a protein binding, and protein homodimerization activity (Fig. 4E). KEGG analysis showed that six core targets were closely related to small cell lung cancer, platinum resistance, the p53 signaling pathway, apoptosis, and other pathways (Fig. 4F). Then the Acacetin-hepatic Fibrosis-Core Target-KEGG network was made (Fig. 4G).

Network pharmacology predicted apoptosis targets and then verified them by molecular docking and signaling pathway experiments.

Potential binding modes and interactions of acacetin with six core targets were investigated by molecular docking. Acacetin binds to the TP53 protein, and the least energetic residue involved in the formation of hydrogen bonds is LEU-25 (−1.56 kcal/mol) (Fig. 5A). According to the CASP3 docking results, the key residue involved in hydrogen bond binding with the lowest energy (−4.54 kcal/mol) was GLY-122 (Fig. 5B). For CASP8 and acacetin binding, SER-402 was the key residue involved in hydrogen bond binding with the lowest energy (−2.47 kcal/mol) (Fig. 5C). For the binding of BCL2 to acacetin, the key residues involved in the hydrogen bond with the lowest energy were GLU-50 and LYS-17 (−2.6 and −2.06 kcal/mol) (Fig. 5D). For PARP1 and acacetin binding, the three key residues with the lowest energies were found to be ALA-219, LYS-232, and LEU-280 (−2.81, −3.58 and −2.79 kcal/mol) (Fig. 5E). For the binding of BAX to acacetin, two key residues with the lowest energy were found to be VAL-316 and ARG-215 (−4.48 and −3.91 kcal/mol), which were involved in hydrogen bonding (Fig. 5F). Molecular docking results showed that acacetin could interact with TP53, CASP3, CASP8, BCL2, PARP1, and BAX to form a tight complex.

4. Discussion

Previous reports have shown that acacetin has a pro-apoptotic effect. For example, acacetin induced mitochondrial ROS-mediated cell death in SW480 and HCT-116 colon cancer cells in a caspase-independent manner [32]. And acacetin induced apoptosis in SJSA and HOS cells by activating the ROS/JNK signaling pathway [33]. It has also been demonstrated that activation of the caspase cascade and the generation of reactive oxygen species can induce apoptosis in human gastric cancer cells [34]. These results suggest that acacetin can promote cell apoptosis, but the potential targets and molecular mechanisms of acacetin in hepatic fibrosis remain unclear. Here, we further investigated the potential mechanisms underlying the improvement of hepatic fibrosis by acacetin using network pharmacological analysis combined with experimental validation and molecular docking.

Our results showed that acacetin ameliorated hepatic fibrosis by inhibiting the proliferation of LX-2 cells and promoting the apoptosis of LX-2 cells through caspase-dependent (both extrinsic and intrinsic) and caspase-independent apoptotic pathways. And acacetin promotes the initiation and expression of p53 and causes the expression of the downstream caspase family of p53 pathway, which eventually leads to apoptosis. The potential targets of acacetin and hepatic fibrosis were obtained through network pharmacology. Among the common targets of acacetin and hepatic fibrosis, TP53, CASP3, CASP8, BCL2, PARP1, and BAX were the most

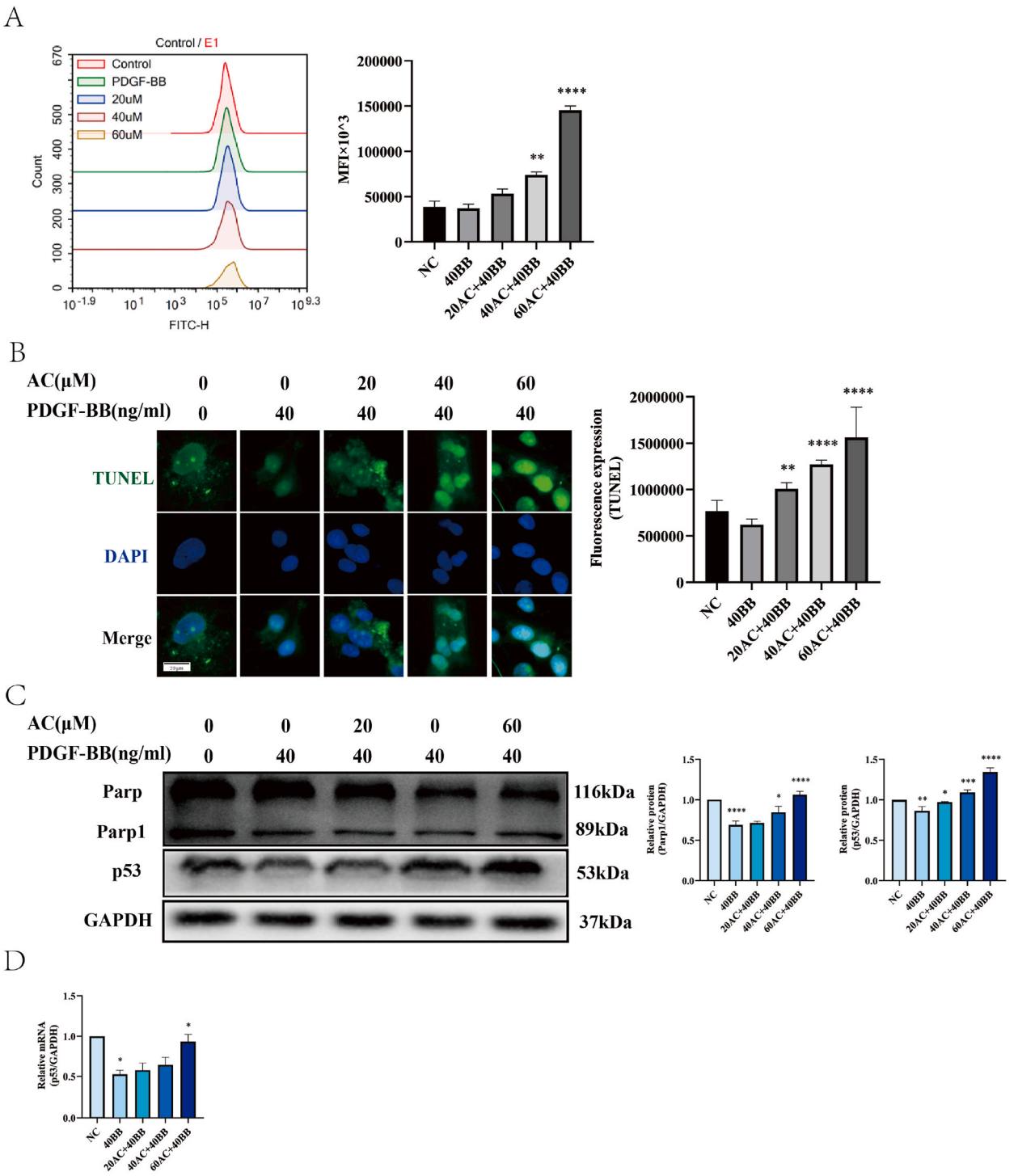

Fig. 3. Acacetin induces apoptosis in LX-2 cells through a caspase-independent pathway, accompanied by ROS generation and P53 activation.(**A**) ROS production in the cells was analyzed by DCFH-DA staining by flow cytometry. (**B**) The level of apoptosis was detected by TUNEL apoptosis staining. (**C**) The protein expression levels of Parp1 and p53 were detected by Western blotting. (**D**) The gene expression level of p53 was determined by QPCR. The data is presented as mean SEM (n = 3). The PDGF-BB stimulation group was compared with the control NC group, and the acacetin drug group was compared with the PDGF-BB stimulation group. Results to * $P < 0.05$, ** $P < 0.01$, *** $P < 0.001$, **** $P < 0.0001$.

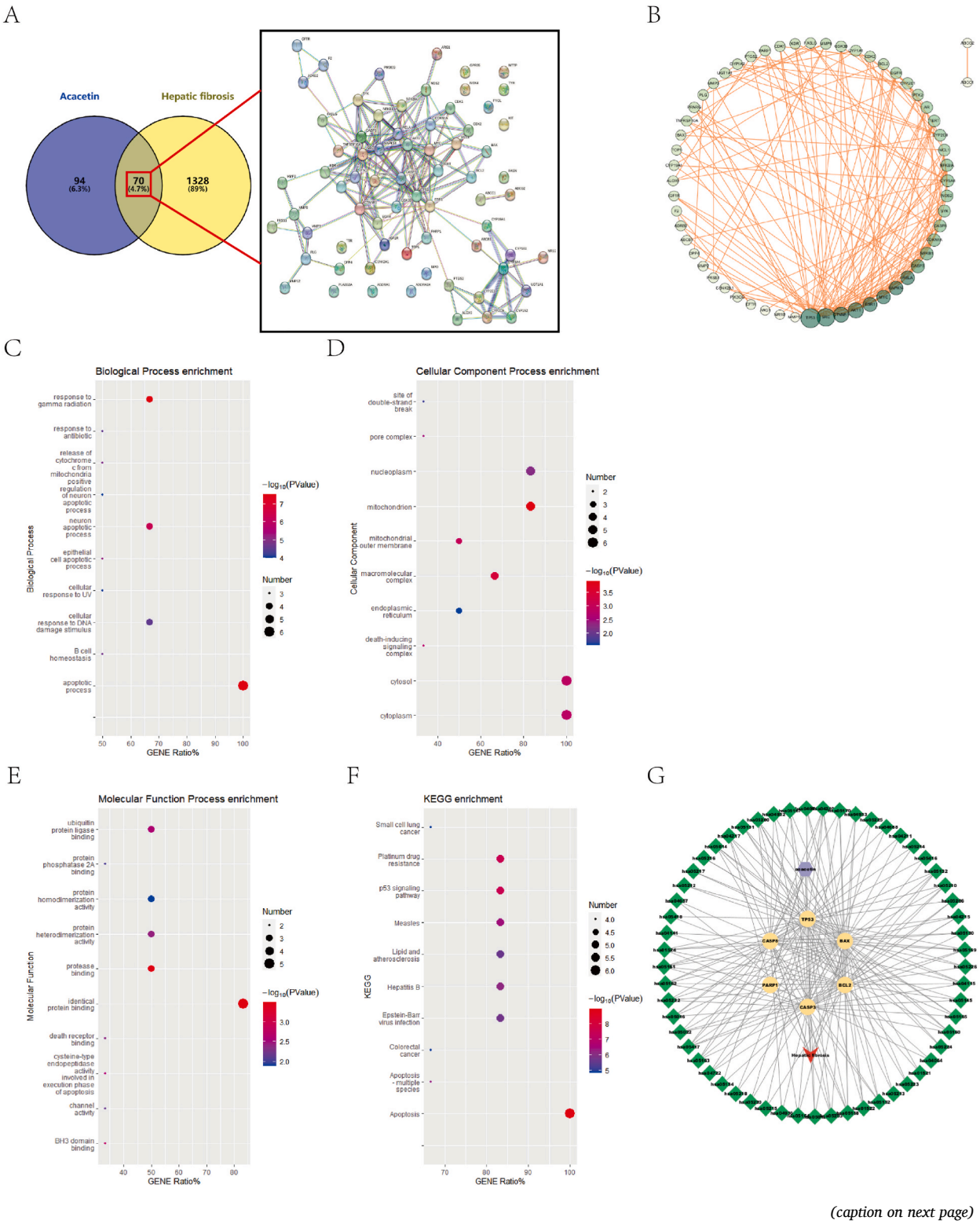

(caption on next page)

Fig. 4. Network pharmacology was used to screen the relationship and mechanism between acacetin and the common core targets of hepatic fibrosis. (**A**) The Venn diagram and PPI network were used to identify all acacetin and hepatic fibrosis targets, as well as 70 cross-targets. (**B**) The protein-protein interaction (PPI) network was constructed by Cytoscape v3.9.1 software and arranged according to the number of nodes and edges of the target sites. (**C-E**) GO analysis of the core targets related to apoptosis showed that the top 10 items related to acacetin, an anti-hepatic fibrosis drug. (**F**) A KEGG pathway analysis of the core targets showed that the top 10 items related to acacetin's anti-hepatic fibrosis activity. (**G**) The network constructed by bioinformatics analysis highlighted the interaction between acacetin and hepatic fibrosis, the core target of the KEGG network. Acacetin is shown in purple hexagons, hepatic fibrosis in red V-shapes, core targets in yellow circles, and KEGG pathways in green diamonds. (For interpretation of the references to colour in this figure legend, the reader is referred to the Web version of this article.)

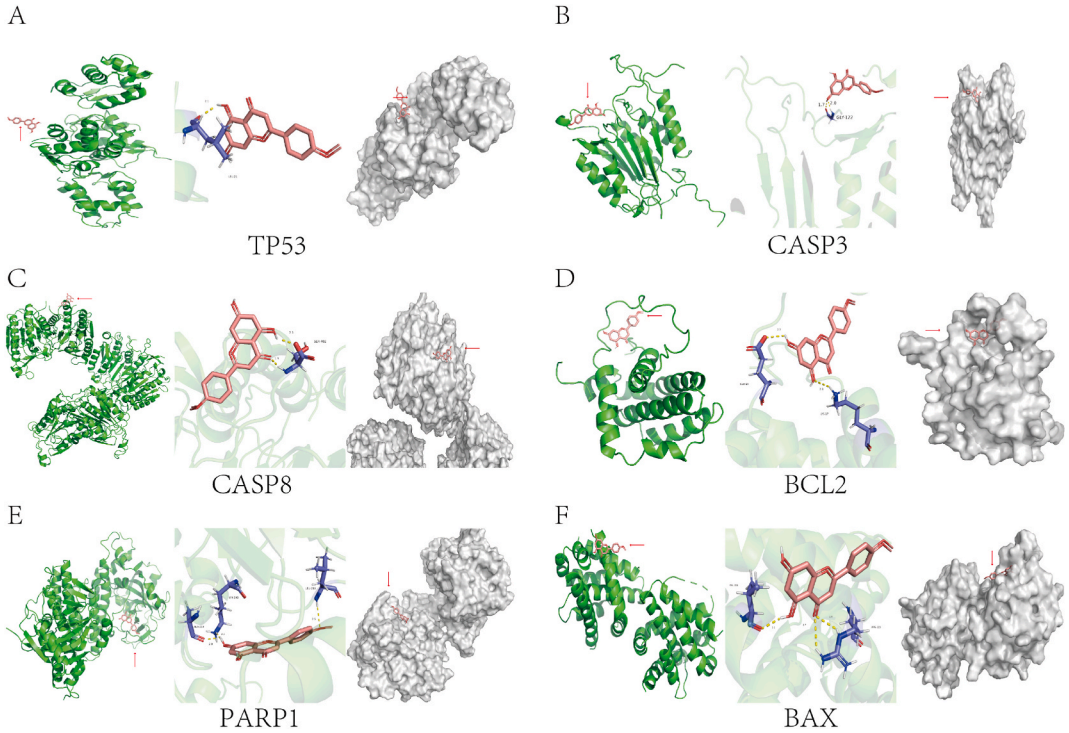

Fig. 5. Network pharmacology predicted apoptosis targets and then verified them by molecular docking and signaling pathway experiments. (**A-F**) The 3D docking of core targets TP53, CASP3, CASP8, BCL2, PARP1, and BAX with acacetin is shown, as are the binding sites and the names of their binding residues, and the 3D docking of the pocket structures of each target with acacetin. The position of acacetin in the figure is indicated by a red arrow; acacetin structure is shown as a red rod; the structure of the target site is shown as a green band; interacting residues are shown as purple rods; connected hydrogen bonds are shown as a yellow short rod target pocket structure (Hydrogen bond is the most stable molecular binding force); and the target mosaic model is shown in gray. (For interpretation of the references to colour in this figure legend, the reader is referred to the Web version of this article.)

important targets related to apoptosis in the PPI network. In the above network pharmacological results, we found that there are common targets of P53 and apoptosis-related proteins in acacetin and liver fibrosis, which further confirmed that acacetin may promote apoptosis in liver fibrosis through P53 pathway. Based on this research, we used molecular docking experiments to simulate the binding between acacetin and P53 and apoptosis-related targets. The amino acid residues binding between acacetin and these targets were verified, and the binding process between acacetin and these targets was visually analyzed. Our results identify LEU-25 as the key TP53 residue in the binding pocket. The tumor protein p53 is a key regulator of several cellular pathways, including DNA repair, cell cycle, and angiogenesis [35]. Our Western blot and real-time quantitative PCR results indicate that P53 activation plays an important role in acacetin promoting apoptosis in LX-2 cells.

GO and KEGG analyses were used to analyze the interactions between multiple targets and pathways. The important targets were subjected to GO and KEGG analysis, and the top 10 enriched biological processes and related signaling pathways were presented. CASP3, CASP8, BCL2, PARP1, and BAX are related to the apoptosis of LX-2 cells mediated by acacetin. In previous studies, apoptosis was an important mechanism by which many drugs achieved anti-tumor effects. It mainly includes caspase-dependent pathways (extrinsic and intrinsic) and caspase-independent pathways [36]. Apoptosis mainly consists of two pathways, one is a Caspase cascade mediated by specific caspase enzymes, such as caspase3. These caspase enzymes play a role in a cascade of reactions, the other being the mitochondrial pathway, which is primarily regulated by members of the Bcl-2 family, including the pro-apoptotic family Bax and the anti-apoptotic family Bcl-2 [37]. Our experiments demonstrated that acacetin induced apoptosis in LX-2 cells by promoting the

activation of the caspase cascade. In addition, ROS has a high biological activity, and excessive ROS can cause oxidative damage to lipids, proteins, and DNA, thereby causing cell apoptosis [31]. Therefore, we investigated the ability of acacetin to induce apoptosis in LX-2 cells through a caspase-independent pathway, accompanied by ROS generation.

In our study, we found that acacetin induced apoptosis in LX-2 cells through multiple ways and pathways, accompanied by ROS generation and activation of the P53 signaling pathway. Most importantly, we verified the binding sites of acacetin to the above targets by network analysis, and acacetin showed good affinity for all the above apoptosis targets. The pathogenesis of liver fibrosis is dynamic and reversible, and if it is not controlled in the early stages, it will develop into cirrhosis. The pathogenesis of liver cirrhosis causes damage to the basic structure of the liver and is considered irreversible in the advanced stage [38]. Therefore, in this study, we only investigated the possibility of promoting apoptosis of hepatic stellate cells in the state of liver fibrosis to achieve the reversal of liver fibrosis. Taken together, these results suggest that acacetin induces apoptosis in LX-2 cells through multiple ways and pathways and that activation of the P53 signaling pathway is involved in this biological process, which is expected to improve hepatic fibrosis. However, our study only verified the possible mechanism of acacetin on liver fibrosis in vitro, and no in vivo drug intervention experiment was performed. We are fully aware that there are still shortcomings, and we will improve them in the follow-up study.

5. Conclusions

Our results indicate that acacetin induces P53 activation and promotes apoptosis of hepatic stellate cells through the caspase cascade and caspase-independent pathway, accompanied by ROS generation, thereby achieving the purpose of ameliorating hepatic fibrosis.

Funding statement

This work was supported by the Sichuan Provincial Administration of Traditional Chinese Medicine (no.2021MS101, 2021MS508) and Center for Healthy Aging, Chengdu Medical College (no. YLZBZ2021, YLZBZ2010).

Data availability statement

Data included in article/supp. material/referenced in article.

CRediT authorship contribution statement

Xue Hu: Writing – original draft, Visualization, Methodology, Investigation. **Haotian Shen:** Writing – original draft, Software, Data curation. **Rong Liu:** Supervision, Formal analysis. **Bin Tang:** Writing – review & editing, Funding acquisition. **Fengmei Deng:** Writing – review & editing, Funding acquisition.

Declaration of competing interest

The authors declare the following financial interests/personal relationships which may be considered as potential competing interests: Fengmei Deng reports financial support was provided by Sichuan Provincial Administration of Traditional Chinese Medicine. Bin Tang reports financial support was provided by Sichuan Provincial Administration of Traditional Chinese Medicine. Bin Tang reports financial support was provided by Center for Healthy Aging, Chengdu Medical College. Fengmei Deng reports financial support was provided by Center for Healthy Aging, Chengdu Medical College. If there are other authors, they declare that they have no known competing financial interests or personal relationships that could have appeared to influence the work reported in this paper.

Appendix A. Supplementary data

Supplementary data to this article can be found online at https://doi.org/10.1016/j.heliyon.2024.e28693.

References

[1] Y. Zhou, R. Wu, F.-F. Cai, W.-J. Zhou, Y.-Y. Lu, H. Zhang, Q.-L. Chen, S.-B. Su, Xiaoyaosan decoction alleviated rat liver fibrosis via the TGFβ/Smad and Akt/FoxO3 signaling pathways based on network pharmacology analysis, J. Ethnopharmacol. 264 (2021) 113021, https://doi.org/10.1016/j.jep.2020.113021.
[2] J. Li, J. Zhang, B. Zhang, L. Chen, G. Chen, D. Zhu, J. Chen, L. Duan, Y. Duan, rSjP40 inhibited the activity of collagen type I promoter via Ets-1 in HSCs, Front. Cell Dev. Biol. 9 (2021) 765616, https://doi.org/10.3389/fcell.2021.765616.
[3] M. Parola, M. Pinzani, Liver fibrosis in NAFLD/NASH: from pathophysiology towards diagnostic and therapeutic strategies, Mol. Aspect. Med. 95 (2024) 101231, https://doi.org/10.1016/j.mam.2023.101231.
[4] D. Xiang, J. Zou, X. Zhu, X. Chen, J. Luo, L. Kong, H. Zhang, Physalin D attenuates hepatic stellate cell activation and liver fibrosis by blocking TGF-β/Smad and YAP signaling, Phytomedicine Int. J. Phytother. Phytopharm. 78 (2020) 153294, https://doi.org/10.1016/j.phymed.2020.153294.
[5] M. Li, Z.Q. Wang, L. Zhang, H. Zheng, D.W. Liu, M.G. Zhou, Burden of cirrhosis and other Chronic liver diseases caused by specific Etiologies in China, 1990-2016: Findings from the Global Burden of disease study 2016, Biomed. Environ. Sci. BES 33 (2020) 1–10, https://doi.org/10.3967/bes2020.001.

[6] S. Mountford, M. Effenberger, H. Noll-Puchta, L. Griessmair, A. Ringleb, S. Haas, G. Denk, F.P. Reiter, D. Mayr, C.A. Dinarello, H. Tilg, P. Bufler, Modulation of liver inflammation and fibrosis by Interleukin-37, Front. Immunol. 12 (2021) 603649, https://doi.org/10.3389/fimmu.2021.603649.

[7] J.-B. Qiao, Q.-Q. Fan, C.-L. Zhang, J. Lee, J. Byun, L. Xing, X.-D. Gao, Y.-K. Oh, H.-L. Jiang, Hyperbranched lipoid-based lipid nanoparticles for bidirectional regulation of collagen accumulation in liver fibrosis, J. Control. Release Off. J. Control. Release Soc. 321 (2020) 629–640, https://doi.org/10.1016/j.jconrel.2020.02.049.

[8] C.-J. Liou, S.-J. Wu, L.-C. Chen, K.-W. Yeh, C.-Y. Chen, W.-C. Huang, Acacetin from Traditionally Used Saussurea involucrata Kar. et Kir. Suppressed Adipogenesis in 3T3-L1 Adipocytes and Attenuated Lipid Accumulation in Obese Mice, Front. Pharmacol. 8 (2017) 589, https://doi.org/10.3389/fphar.2017.00589.

[9] S. Singh, P. Gupta, A. Meena, S. Luqman, Acacetin, a flavone with diverse therapeutic potential in cancer, inflammation, infections and other metabolic disorders, Food Chem. Toxicol. Int. J. Publ. Br. Ind. Biol. Res. Assoc. 145 (2020) 111708, https://doi.org/10.1016/j.fct.2020.111708.

[10] M. Alfwuaires, H. Elsawy, A. Sedky, Acacetin inhibits cell proliferation and induces apoptosis in human hepatocellular carcinoma cell lines, Mol. Basel Switz. 27 (2022), https://doi.org/10.3390/molecules27175361.

[11] F. Sun, D. Li, C. Wang, C. Peng, H. Zheng, X. Wang, Acacetin-induced cell apoptosis in head and neck squamous cell carcinoma cells: Evidence for the role of muscarinic M3 receptor, Phytother. Res. PTR 33 (2019) 1551–1561, https://doi.org/10.1002/ptr.6343.

[12] J.Y. Lee, D.Y. Jun, K.Y. Kim, E.J. Ha, M.H. Woo, J.Y. Ko, Y.H. Yun, I.-S. Oh, Y.H. Kim, Pharmacologic inhibition of autophagy sensitizes human acute leukemia Jurkat T cells to acacetin-induced apoptosis, J. Microbiol. Biotechnol. 27 (2017) 197–205, https://doi.org/10.4014/jmb.1610.10055.

[13] P. Li, X. Gong, L. Yuan, L. Mu, Q. Zheng, H. Xiao, H. Wang, Palmitoylation in apoptosis, J. Cell. Physiol. 238 (2023) 1641–1650, https://doi.org/10.1002/jcp.31047.

[14] M. Lacroix, R. Riscal, G. Arena, L.K. Linares, L. Le Cam, Metabolic functions of the tumor suppressor p53: implications in normal physiology, metabolic disorders, and cancer, Mol. Metabol. 33 (2020) 2–22, https://doi.org/10.1016/j.molmet.2019.10.002.

[15] Y. Dong, Q. Zhao, Y. Wang, Network pharmacology-based investigation of potential targets of astragalus membranaceous-angelica sinensis compound acting on diabetic nephropathy, Sci. Rep. 11 (2021) 19496, https://doi.org/10.1038/s41598-021-98925-6.

[16] Y. Ouyang, Y. Rong, Y. Wang, Y. Guo, L. Shan, X. Yu, L. Li, J. Si, X. Li, K. Ma, A systematic study of the mechanism of acacetin against sepsis based on network pharmacology and experimental validation, Front. Pharmacol. 12 (2021) 683645, https://doi.org/10.3389/fphar.2021.683645.

[17] X. Guo, Y. Xu, H.-L. Tan, X.-J. Wang, L. Xiao, The key ingredient acacetin in Weishu decoction alleviates gastrointestinal motility disorder based on network pharmacology analysis, Mediat. Inflamm. 2021 (2021) 5265444, https://doi.org/10.1155/2021/5265444.

[18] C. Li, Y.H. Tan, J. Sun, F.M. Deng, Y.L. Liu, PAX6 contributes to the activation and proliferation of hepatic stellate cells via activating Hedgehog/GLI1 pathway, Biochem. Biophys. Res. Commun. 526 (2020) 314–320, https://doi.org/10.1016/j.bbrc.2020.03.086.

[19] M.-W. Kong, Y. Gao, Y.-Y. Xie, E.-H. Xing, L.-X. Sun, H.-J. Ma, H.-Y. Xing, Mechanism of GLP-1 receptor agonists-mediated attenuation of palmitic acid-induced Lipotoxicity in L6 Myoblasts, BioMed Res. Int. 2022 (2022) 6237405, https://doi.org/10.1155/2022/6237405.

[20] B. Yao, S. Zhu, X. Wei, M.-K. Chen, Y. Feng, Z. Li, X. Xu, Y. Zhang, Y. Wang, J. Zhou, N. Tang, C. Ji, P. Jiang, S.-C. Zhao, C. Qin, N. Feng, The circSPON2/miR-331-3p axis regulates PRMT5, an epigenetic regulator of CAMK2N1 transcription and prostate cancer progression, Mol. Cancer 21 (2022) 119, https://doi.org/10.1186/s12943-022-01598-6.

[21] M. Xu, X. Chen, K. Lin, K. Zeng, X. Liu, B. Pan, X. Xu, T. Xu, X. Hu, L. Sun, B. He, Y. Pan, H. Sun, S. Wang, The long noncoding RNA SNHG1 regulates colorectal cancer cell growth through interactions with EZH2 and miR-154-5p, Mol. Cancer 17 (2018) 141, https://doi.org/10.1186/s12943-018-0894-x.

[22] Y. Tan, C. Li, J. Zhou, F. Deng, Y. Liu, Berberine attenuates liver fibrosis by autophagy inhibition triggering apoptosis via the miR-30a-5p/ATG5 axis, Exp. Cell Res. 427 (2023) 113600, https://doi.org/10.1016/j.yexcr.2023.113600.

[23] S. Miura, K. Katayama, Y. Sugimoto, F. Tanaka, M. Mori, D. Takahashi, R. Saiki, Y. Hirabayashi, T. Murata, I. Tawara, K. Dohi, Discordance of light chain isotypes between serum and glomerular deposits in proliferative glomerulonephritis with monoclonal IgG deposits: a case report and review of the literature, BMC Nephrol. 24 (2023) 199, https://doi.org/10.1186/s12882-023-03256-5.

[24] Y. Ren, A. Wang, D. Wu, C. Wang, M. Huang, X. Xiong, L. Jin, W. Zhou, Y. Qiu, X. Zhou, Dual inhibition of innate immunity and apoptosis by human cytomegalovirus protein UL37x1 enables efficient virus replication, Nat. Microbiol. 7 (2022) 1041–1053, https://doi.org/10.1038/s41564-022-01136-6.

[25] B. Zhao, L. Zeng, D. Chen, S. Xie, Z. Jin, G. Li, W. Tang, Q. He, NIR-photocatalytic regulation of arthritic synovial microenvironment, Sci. Adv. 8 (2022) eabq0959, https://doi.org/10.1126/sciadv.abq0959.

[26] Z. Miao, W. Tian, Y. Ye, W. Gu, Z. Bao, L. Xu, G. Sun, C. Li, Y. Tu, H. Chao, S.M. Lam, N. Liu, J. Ji, Hsp90 induces Acsl4-dependent glioma ferroptosis via dephosphorylating Ser637 at Drp1, Cell Death Dis. 13 (2022) 548, https://doi.org/10.1038/s41419-022-04997-1.

[27] Y. Guo, Q. Zhang, Q. Zhu, J. Gao, X. Zhu, H. Yu, Y. Li, C. Zhang, Copackaging photosensitizer and PD-L1 siRNA in a nucleic acid nanogel for synergistic cancer photoimmunotherapy, Sci. Adv. 8 (2022) eabn2941, https://doi.org/10.1126/sciadv.abn2941.

[28] Y. Zhang, F. Lu, Molecular mechanism of triptolide in myocardial fibrosis through the Wnt/β-catenin signaling pathway, Scand. Cardiovasc. J. SCJ 58 (2024) 2295785, https://doi.org/10.1080/14017431.2023.2295785.

[29] X.-M. Hu, S. Zheng, Q. Zhang, X. Wan, J. Li, R. Mao, R. Yang, K. Xiong, PANoptosis signaling enables broad immune response in psoriasis: from pathogenesis to new therapeutic strategies, Comput. Struct. Biotechnol. J. 23 (2024) 64–76, https://doi.org/10.1016/j.csbj.2023.11.049.

[30] M. Zhu, J. Qu, Q. Deng, Identification of potential inhibitors against Staphylococcus aureus shikimate dehydrogenase through virtual screening and susceptibility test, J. Enzym. Inhib. Med. Chem. 39 (2024) 2301768, https://doi.org/10.1080/14756366.2024.2301768.

[31] U.S. Srinivas, B.W.Q. Tan, B.A. Vellayappan, A.D. Jeyasekharan, ROS and the DNA damage response in cancer, Redox Biol. 25 (2019) 101084, https://doi.org/10.1016/j.redox.2018.101084.

[32] N. Prasad, J.R. Sharma, U.C.S. Yadav, Induction of growth cessation by acacetin via β-catenin pathway and apoptosis by apoptosis inducing factor activation in colorectal carcinoma cells, Mol. Biol. Rep. 47 (2020) 987–1001, https://doi.org/10.1007/s11033-019-05191-x.

[33] S. Wang, B. Lin, W. Liu, G. Wei, Z. Li, N. Yu, X. Xue, G. Ji, Acacetin induces apoptosis in human Osteosarcoma cells by Modulation of ROS/JNK activation, Drug Des. Dev. Ther. 14 (2020) 5077–5085, https://doi.org/10.2147/DDDT.S275148.

[34] M.-H. Pan, C.-S. Lai, P.-C. Hsu, Y.-J. Wang, Acacetin induces apoptosis in human gastric carcinoma cells accompanied by activation of caspase cascades and production of reactive oxygen species, J. Agric. Food Chem. 53 (2005) 620–630, https://doi.org/10.1021/jf048430m.

[35] R. Napolitano, S. De Matteis, S. Carloni, S. Bruno, G. Abbati, L. Capelli, M. Ghetti, M.T. Bochicchio, C. Liverani, L. Mercatali, D. Calistri, A. Cuneo, K. Menon, G. Musuraca, G. Martinelli, G. Simonetti, Kevetrin induces apoptosis in TP53 wild-type and mutant acute myeloid leukemia cells, Oncol. Rep. 44 (2020) 1561–1573, https://doi.org/10.3892/or.2020.7730.

[36] Z.-J. Ma, L. Lu, J.-J. Yang, X.-X. Wang, G. Su, Z.-L. Wang, G.-H. Chen, H.-M. Sun, M.-Y. Wang, Y. Yang, Laricresinol induces apoptosis in HepG2 cells via mitochondrial-mediated apoptosis pathway, Eur. J. Pharmacol. 821 (2018) 1–10, https://doi.org/10.1016/j.ejphar.2017.12.027.

[37] S. Nagata, Apoptosis and clearance of apoptotic cells, Annu. Rev. Immunol. 36 (2018) 489–517, https://doi.org/10.1146/annurev-immunol-042617-053010.

[38] A. Smith, K. Baumgartner, C. Bositis, Cirrhosis: diagnosis and management, Am. Fam. Physician 100 (2019) 759–770.